Nonlocal-in-time finite-velocity diffusion approach on a ring

Manuel O. Cáceres [1,2,*] and Guillermo Hansen [3]
[1] *Comision Nacional de Energia Atomica, Centro Atomico Bariloche and Instituto Balseiro, Universidad Nacional de Cuyo, Av. E. Bustillo 9500, CP8400, Bariloche, Argentina*
[2] *CONICET, Centro Atomico Bariloche, CP8400, Bariloche, Argentina*
[3] *Instituto Balseiro, Universidad Nacional de Cuyo, CP8400, Bariloche, Argentina*

(Received 2 April 2024; revised 13 June 2024; accepted 7 August 2024; published 30 August 2024)

The ubiquitous telegrapher's equation is presented in the context of a non-local-in-time master equation on the lattice. From the exact solution of this transport equation, for different hopping models, the second moment in the infinite lattice and the time evolution of the probability in the ring have been analyzed as a function of the two characteristic timescales appearing in the memory kernel of the finite-velocity approach: the rate of energy loss and the timescale characterizing the jumping process in the lattice. We have demonstrated how these timescales characterize the constraint to find positive solutions, the time variation of entropy and therefore the approach to the disordered stationary state on the ring. This lattice model provides an analytic treatment. Thus, this result is relevant in the study of Shannon entropy, transport of information, and waves in lattices and sheds light on the functional role of the loss of energy in the finite-velocity diffusion dynamics.

DOI: 10.1103/PhysRevE.110.024141

I. INTRODUCTION

The telegrapher's equation (TE) was originally introduced by Thomson (Lord Kelvin) in 1854 [1], when he was studying the dissipation of electromagnetic fields in waveguides [2–5]. Nearly one century later, in order to overcome the issue of infinitely fast propagation in a diffusion process, Cattaneo in 1948 proposed to modify the Fourier-Fick law, which led to the TE as well [6,7]. In an early discussion, in the context of relativistic heat transport, Van Kampen used a microscopic model consisting of an ensemble of particles that exchange electromagnetic radiation to derive a memory-like equation from which the TE was an approximation [8]. On the other hand, a pioneering work on hyperbolic diffusion from a discrete point of view was introduced by Goldstein in 1951 [9], from which many generalizations in the context of persistent random walk [10–12] were later implemented. In particular, Kac proved in 1974 that the solution of the TE can be written as a path integral [13]. Therefore, his formula was a direct counterpart of the Feynman-Kac formula for the solution of the ordinary diffusion equation.

Let us point out that, since the inception of these pioneering papers and over many decades, the TE in continuous media: $[\partial_t^2 + \frac{1}{\tau}\partial_t - v^2\partial_x^2]P(x,t) = 0$ has found application in numerous contexts with diverse initial conditions [14]. We first note that the TE has two parameters: the rate of absorption of energy τ^{-1} and the velocity of propagation v. Both parameters can be related to physical constants [2–4,8,15].

For the transport of electromagnetic waves, the TE provides the correct description considering the Joule effect through continuous media. For the transport at finite velocity of heat, photon migration in continuous media, and other similar phenomena, the TE is an improvement over the diffusion limitations. Here we mention a few notable applications:

(i) transmission of electrical signals [2,4,5,16,17],
(ii) hyperbolic diffusion in random media and the persistent random walk [11,12,15,18–20],
(iii) heat transport, Bénard convection and propagation of waves [7,12,21–25],
(iv) high-energy ion collision experiments [26],
(v) waves, dissipation and penetration [27–30],
(vi) relativistic Brownian motion and cosmic microwave background radiation [8,31–35],
(vii) turbulent diffusion and geophysics [36–39],
(viii) surface gravity waves on a random bottom [40,41],
(ix) neutron diffusion and engineering problems [42–46],
(x) Boltzmann-Lorentz random collision models [47–50],
(xi) biophysics and neuroscience [51–55],
(xii) information theory in continuous hyperbolic diffusion [56,57],
(xiii) fractal hyperbolic diffusion [58,59].

It is interesting to note that the solution of the one-dimensional TE can be written as a sum over stochastic trajectories $x(t)$ of the Poisson-Kac flights [13]. Notably, these realizations $x(t)$ are random trajectories of a particle moving with constant velocity but changing direction $\pm v$ due to collisions at random times characterized by a Poisson statistics with mean τ. Generalizations to these path integral approaches have also recently been presented [51,60].

In this work, we extend the hyperbolic diffusion approach to the context of a non-local-in-time master equation on the lattice to study transport on the ring. In this manner, we obtain an exact polynomial solution. The applications of these results are circumscribed to finite systems as occurs in solid-state physics [61,62] and biophysics [38,53,55,63]. We utilize

*Contact author: caceres@cab.cnea.gov.ar

generic transition matrices to describe various jumps on the lattice. Subsequently, we compute the Shannon entropy and investigate the transition to the uniform distribution as a function of the problem's timescales and the parameters that define the hopping on the lattice. The velocity of Shannon entropy shows the crossover from ballistic to diffusive motion.

The organization of the paper is as follows: In Sec. II, we present the finite-velocity transport approach in the lattice as a non-local-in-time difference equation for a generic wave-diffusion-like process. In Sec. III we calculate analytically the second moment for the finite-velocity transport on an infinite lattice. In Sec. IV, we apply this approach to study the finite-velocity transport process on a ring. In Sec. V, we study the Shannon entropy to characterize the loss of information for different hopping models on the ring. These results are obtained analytically for a lattice TE. Finally, in Sec. VI, we discuss the conclusions of the present approach, as well as its future extensions and applications. Appendix A is used to present the memory kernel from the renewal theory to characterize the constraint for the timescale parameters of the memory kernel to obtain positive solutions. Appendix B is dedicated to presenting the nonhomogeneous TE in the continuous limit.

II. THE FINITE-VELOCITY FORMALISM IN A LATTICE TRANSPORT EQUATION

A. The approach to non-local-in-time transport

Consider a specific form of non-local-in-time master equation (ME) [8,50,64,65]:

$$\partial_t P_s(t) = \alpha^2 \int_0^t e^{-(t-t')/\tau} \sum_{s' \in \mathcal{D}_s} \mathbf{H}_{ss'} P_{s'}(t')\, dt', \tag{1}$$

here $P_s(t) \equiv P_s(t|s_0, 0)$ is the conditional probability at time $t_0 = 0$ (site $s_0 \in \mathcal{D}_s$ the lattice domain). We note that (1) is the standart equation of the well-familiar continuous-time random-walk (CTRW) model with the exponential memory kernel [64]. The initial condition $\partial_t P_s(t)|_{t=0} = 0$ is implied by the ME itself.

The occurrence of a memory like the one appearing in (1) can be found coming from the eliminations of variables using projector operator techniques [12,66,67]. Therefore, the IC $\partial_t P_s(t)|_{t=0}$ is related to the mesoscopic preparation of the system before the elimination of variables [8]. We remark that the vector $P_s(t)$, the matrix elements $\mathbf{H}_{ss'}$, and the lattice space s are dimensionless quantities. Here, $\mathbf{H}_{ss'}$ is the lattice transition matrix which can be written in terms of a generic Markov matrix $\mathbf{T}_{ss'}$ (with $\mathbf{T}_{ss'} \geqslant 0$, $\sum_s \mathbf{T}_{ss'} = 1$), and the identity $\mathbf{I}$ in the form:

$$\mathbf{H} = \mathbf{T} - \mathbf{I}. \tag{2}$$

Thus, the matrix $\mathbf{H}$ characterizes the gain-loss form of the ME and fulfils the fundamental conditions:

$$\mathbf{H}_{ss'} \geqslant 0 \text{ if } s \neq s' \text{ and } \sum_{s \in \mathcal{D}_s} \mathbf{H}_{ss'} = 0, \forall s' \in \mathcal{D}_s, \tag{3}$$

where $\mathcal{D}_s$ is the domain of interest.

Now we denote the memory kernel in (1) as:

$$\Phi(t) = \alpha^2 e^{-t/\tau} \text{ with } \alpha \in \mathbb{R},\ \tau > 0, \tag{4}$$

where α^{-1} and τ are timescales that will be characterized in the next sections.

We note that the solution of (1) can be associated with probability theory only if the kernel $\Phi(t)$ fulfills the condition:

$$2\alpha\tau < 1. \tag{5}$$

By construction, the Markov matrix $\mathbf{T}$ generates a positive solution $\mathbf{T}^n$ for discrete times n. Thus, using renewal theory [68], it is possible to introduce the continuous-time representation: $\mathbf{T}^n \to \mathbf{W}(t)$. The important point is that to do this continuous-time prolongation the parameters (α, τ) must fulfill the condition (5). In Appendix A, we deduce this bound and the connection of the kernel with the waiting-time density function $\psi(t)$ of the renewal theory in a diffusion-like approach [61,69].

B. The generalized finite-velocity lattice transport approach

From the non-local-in-time ME (1), we can get a generalized finite-velocity diffusion equation. By taking the time derivative on (1) we obtain:

$$\partial_t^2 P_s(t) = \alpha^2 \sum_{s' \in \mathcal{D}_s} \mathbf{H}_{ss'} P_{s'}(t') - \frac{\alpha^2}{\tau} \int_0^t e^{-(t-t')/\tau} \sum_{s' \in \mathcal{D}_s} \mathbf{H}_{ss'} P_{s'}(t')\, dt'. \tag{6}$$

Therefore, arriving at the generalized lattice TE as shown in Ref. [64],

$$\partial_t^2 P_s(t) + \frac{1}{\tau} \partial_t P_s(t) = \alpha^2 \sum_{s' \in \mathcal{D}_s} \mathbf{H}_{ss'} P_{s'}(t). \tag{7}$$

This second-order in time equation contains both ingredients that lead to wave and diffusion transport. In fact the competition between the timescales τ, α^{-1}, and the time process t gives rise to the crossover ballistic-diffusion in the analysis of the behavior of the conditional probability $P_s(t)$ under the restriction (5). That is, the fine-velocity diffusion approach. In the lattice framework, this equation can be extended to arbitrary dimensions by considering a spatial vector s. This situation is different when deducing, in the "fluid limit," the continuous TE from the persistent random walk in higher dimensions. This problem under the isotropic and uniform restriction has been solved using a multistate random walk defined on a continuous set of angular values [70].

Specific models for the transition matrix $\mathbf{H}$ characterize different evolutions on the lattice. In particular, two extreme limits will be presented in the context of pure wave evolution, as well as pure diffusion transport in the lattice. In general, in the Fourier and Laplace representations, the solution of (7) on the lattice can be found due to the space translational invariance. Therefore, the competition between the finite-velocity behavior and different jump models could be studied in this context. In addition, from this equation we will show that the timescale τ is related to relaxation, while the timescale α^{-1} is related to the transport of information in the process. This will be presented in subsection D and in Appendix A for the two different limits: wavelike and diffusion-like cases.

If the space is continuous, then $\mathbf{H}$ can be an integral or a differential operator, as shown below. In this case, a natural dimension of length appears.

1. Generic solution of (7)

By introducing discrete Fourier and Laplace transforms:

$$P_k(u) \equiv \sum_{s=-\infty}^{\infty} e^{iks} \int_0^{\infty} e^{-ut} P_s(t) dt, \tag{8}$$

into (7) we obtain

$$u^2 P_k(u) - uP_k(t)|_{t=0} - \partial_t P_k(t)|_{t=0} + \tau^{-1}[uP_k(u) - P_k(t)|_{t=0}] = \alpha^2 (T(k) - 1) P_k(u), \tag{9}$$

where $T(k)$ is the Fourier transform of the transition probability, $\mathbf{T}_{ss'}$, from site s' to s, that is:

$$T(k) = \sum_{s=-\infty}^{\infty} e^{ik(s-s')} \mathbf{T}_{ss'},$$

and its Fourier inverse:

$$\mathbf{T}_{ss'} \equiv \frac{1}{2\pi} \int_0^{2\pi} dk\, e^{-ik(s-s')} T(k). \tag{10}$$

Introducing short notation for the IC

$$P_k(t)|_{t=0} \equiv P_k(0) \quad \text{and} \quad \partial_t P_k(t)|_{t=0} \equiv \dot{P}_k(0), \tag{11}$$

and solving for $P_k(u)$, we obtain:

$$P_k(u) = \frac{(u + \tau^{-1}) P_k(0)}{u(u + \tau^{-1}) + \alpha^2 (1 - T(k))}. \tag{12}$$

From this formula we readily see that all the information rest on the Fourier representation $T(k)$ of the probability transition matrix $\mathbf{T}$.

Finding the poles of (12)

$$u_{\pm} \equiv u_{\pm}(k) = \frac{1}{2\tau}[-1 \pm \sqrt{1 - (2\tau\alpha)^2 (1 - T(k))}]. \tag{13}$$

The Laplace inversion of the solution (12)

$$P_k(t) = \frac{1}{2\pi i} \int_{c-i\infty}^{c+i\infty} du\, e^{ut} P_k(u), \tag{14}$$

gives

$$P_k(t) = P_k(0) \left[\frac{1}{\tau} \left(\frac{e^{tu_+} - e^{tu_-}}{u_+ - u_-} \right) + \left(\frac{u_+ e^{tu_+} - u_- e^{tu_-}}{u_+ - u_-} \right) \right], \tag{15}$$

where we have used the intrinsic IC $\partial_t P_k(t)|_{t=0} = 0$ appearing in (1). In order to remove this initial condition, it is necessary to modify the non-local-in-time ME (1) to allow for an arbitrary IC $\partial_t P_k(t)|_{t=0} \neq 0$. This can be done, but the resulting differential equation will have a nonhomogeneous term. In Appendix B we present this discussion for the continuous case and compare the solution with the one from the ordinary (homogeneous) TE.

C. Two extreme limits

1. Wave limit

Starting from the non-local-in-time transport equation (1), two extreme limits can easily be found. First, by taking the limit $\tau \to \infty$ in (1), we arrive at the following equation:

$$\partial_t P_s(t) = \alpha^2 \int_0^t \sum_{s' \in \mathcal{D}_s} \mathbf{H}_{ss'} P_{s'}(t')\, dt'. \tag{16}$$

From (16) and taking the time derivative, we obtain a lattice wavelike equation:

$$\partial_t^2 P_s(t) = \alpha^2 \sum_{s' \in \mathcal{D}_s} \mathbf{H}_{ss'} P_{s'}(t),$$

the evolution of this equation will be dominated by the transition matrix $\mathbf{H} = \mathbf{T} - \mathbf{1}$. The solution of this equation can be found by taking the limit $\tau \to \infty$ in (12). Thus, the inversion in Laplace gives the result

$$P_k(t) = P_k(0) \cos[\alpha \sqrt{1 - T(k)} t], \tag{17}$$

where we have used $\dot{P}_k(0) = 0$. Unfortunately, obtaining analytical solutions in the s space is not possible because the Fourier inversion cannot be performed analytically, even for the simplest model of the nearest-neighbor transition structure $T(k)$.

Lattice wave localization in the presence of disorder and a plethora of experimental investigations involving time and length scales can be studied from this approach. The space-continuous limit can be seen in Ref. [29]. We note that the limit $\tau \to \infty$ does not fulfill (A1), so a waiting-time probability density $\psi(t)$ does not exist for this wave-limit case. In Appendix A, we define the function $\psi(t)$ in the renewal context for a continuous-time representation of a Markov chain, which is a diffusion-like process [by construction a positive solution $P_s(t)$].

2. Diffusion limit

In the opposite case, by taking $\tau \to 0$ and $\alpha \to \infty$ such that $\alpha^2 \tau \to \lambda$ in (1), we recover the usual lattice diffusion transport:

$$\partial_t P_s(t) = \lambda \int_0^t \delta(t - t') \sum_{s' \in \mathcal{D}_s} \mathbf{H}_{ss'} P_{s'}(t')\, dt' = \lambda \sum_{s' \in \mathcal{D}_s} \mathbf{H}_{ss'} P_{s'}(t). \tag{18}$$

This is a lattice diffusion equation characterized by the transition matrix $\mathbf{H}$. The solution to this equation can be found by taking the limit $\tau \to 0$ and $\alpha \to \infty$ such that $\alpha^2 \tau \to \lambda$ in (12). Thus, the inversion in Laplace gives the familiar result [12,62],

$$P_k(t) = P_k(0) \exp(-\lambda(1 - T(k))t). \tag{19}$$

To our knowledge, Fourier inversion can only be done analytically for the simplest model of the nearest-neighbor transition structure $T(k)$ [12].

D. Wavy perturbation solution

To understand the meaning of the parameters $\{\alpha, \tau\}$ appearing in (7), we introduce a perturbation analysis in the wavelike limit. First, we rewrite the Fourier representation of (7) in the form

$$\mathbf{H}(k)P_k(t) = \frac{1}{\alpha^2}\left(\partial_t^2 P_k(t) + \frac{1}{\tau}\partial_t P_k(t)\right). \tag{20}$$

Now we propose a solution of the form

$$P_k(t) = e^{-t/2\tau} f(k,t). \tag{21}$$

Substitution of this ansatz in (20) leads to a function f satisfying

$$\mathbf{H}(k)f(k,t) = \frac{1}{\alpha^2}\left(\partial_t^2 f(k,t) - \left(\frac{1}{2\tau}\right)^2 f(k,t)\right). \tag{22}$$

Because $(1/\tau)$ is a small quantity, (22) can be approximated by a lattice wave equation to order $\mathcal{O}(\tau^{-2})$, so (21) is the perturbative solution of (20). Here $e^{-t/2\tau}$ is an attenuation factor. Thus, τ is the timescale related to the dissipation and the timescale α^{-1} is related to the velocity in the wave motion (solution $f(k,t)$).

In addition to the result (21), let us introduce a perturbation in the small parameter τ^{-1} from the exact solution (15). Considering the behavior of the poles (13) up to $\mathcal{O}(\tau^{-2})$, we obtain the final expression to $\mathcal{O}(\tau^{-1})$:

$$\frac{P_k(t)}{P_k(0)} = \left\{1 - \frac{t}{2\tau}\right\}\cos(\alpha\sqrt{1-T(k)}t) + \frac{\sin(\alpha\sqrt{1-T(k)}t)}{\sqrt{1-T(k)}}\frac{1}{2\alpha\tau} + \mathcal{O}(\tau^{-2}). \tag{23}$$

From this result, important conclusions can be drawn. The first contribution in the right-hand side of (23) corresponds to the expansion of (21) and is in accordance with the pure wave solution (17). The second contribution depends on the group of parameters $2\alpha\tau$, and its time dependence is purely oscillatory. It is interesting to note that from this characteristic function, it is difficult to apply Bochner's theorem [12,62,68] to prove the positivity of the inverse Fourier transform: $P_s(t)$. We have checked numerically that for certain jump structures $T(k)$ and values of the group $2\alpha\tau > 1$, the inverse Fourier transform $P_s(t)$ is not positive for some values of time t. This phenomenon will be illustrated in Figs. 1 and 2 of Sec. IV B.

The analysis to interpret the parameters $\{\alpha, \tau\}$ in a diffusion-like case (positive $P_s(t)$) is presented in Appendix A and leads to the condition $2\alpha\tau < 1$.

E. On the transition matrices T and H

1. n-step discrete models

The ME operator $\mathbf{H} = \mathbf{T} - \mathbf{I}$ entirely characterizes the transition process. This ME operator can be written in terms of the probability matrix $\mathbf{T}$. A general transition (n-step) matrix $\mathbf{T}$ can be written in terms of step operators $\mathbf{E}^{\pm}$. These operators are defined by their action on any vector f_s, producing a translation of the form:

$$\mathbf{E}^{\pm n} f_s = f_{s\pm n}. \tag{24}$$

Then, a symmetric n-step jump model can be written in the generic form:

$$\mathbf{T} = \mathcal{C}\sum_{n=1}^{\mathcal{N}} p_n(\mathbf{E}^{+n} + \mathbf{E}^{-n}), \tag{25}$$

where C is a normalization constant, $\mathcal{N}$ characterizes a particular n-step model, and p_n is the probability of occurrence of an n-step jump on the lattice. Other models can be worked out in a similar way, as we show below.

2. Continuous models

We can work out a series for the translational operator:

$$\mathbf{E}^{\pm} \equiv e^{\pm\partial_s} = 1 \pm \partial_s + \frac{1}{2!}\partial_s^2 \pm \frac{1}{3!}\partial_s^3 + \cdots. \tag{26}$$

Introducing a lattice parameter, denoted by ϵ, and using the change of variables $x = \epsilon s$ from (26), we arrive at the series expansion

$$\mathbf{E}^{\pm} \equiv e^{\pm\epsilon\partial_x} = 1 \pm \epsilon\partial_x + \frac{\epsilon^2}{2!}\partial_x^2 \pm \frac{\epsilon^3}{3!}\partial_x^3 + \cdots.$$

Thus, for the symmetric case, when the lattice parameter goes to zero, we get the continuous limit for the ME operator $\mathbf{H}$:

$$\lim_{\epsilon\to 0}\sum_{s'\in\mathcal{D}_s}\mathbf{H}_{ss'}f_{s'} \to \epsilon^2 p_1\partial_x^2 f(x) + \mathcal{O}(\epsilon^4). \tag{27}$$

Here f_s is any vector on $\mathcal{D}_s$ and $f(x)$ is its continuous prolongation. In particular, if the model for $\mathbf{H}$ has only transitions to the first-neighboring sites, then we take $p_1 = \frac{1}{2}$.

Asymmetric models can be adjusted by considering different probabilities for the jump to the left and right in the form: $p_n\mathbf{E}^{+n} + q_n\mathbf{E}^{-n}$. Models like these will produce a bias in a privileged direction, leading in the continuous limit to a dominant term of the form proportional to $\epsilon\partial_x f(x)$, etc.

Other, more complex space jump models can also be introduced in a similar way. For example, in the context of a continuous space model, using the integral operator [63]:

$$\sum_{s'\in\mathcal{D}_s}\mathbf{H}_{ss'}f_{s'} \to \frac{\text{const}}{\pi}\sin(\pi\mu/2)\Gamma(\mu+1) \times \int_{-\infty}^{+\infty} dx' \frac{f(x')}{|x-x'|^{\mu+1}}, \tag{28}$$

with $0 < \mu < 2$. It is possible to prove that this ME operator is the continuous version of the Weierstrass model, see below. An expansion of the transition operator (28) in a Kramers-Moyal series leads to derivative terms of all orders. Nevertheless, this series cannot be truncated at any order. Other finite-velocity transport equations can also be obtained using different models for the ME operator $\mathbf{H}$ in (1); these will be presented in the next sections.

3. Transition with the next-nearest-neighbor jump model

From (25), the simplest case corresponds to a model with transitions only to first neighbors:

$$\mathbf{T} = \tfrac{1}{2}(\mathbf{E}^{+} + \mathbf{E}^{-}), \tag{29}$$

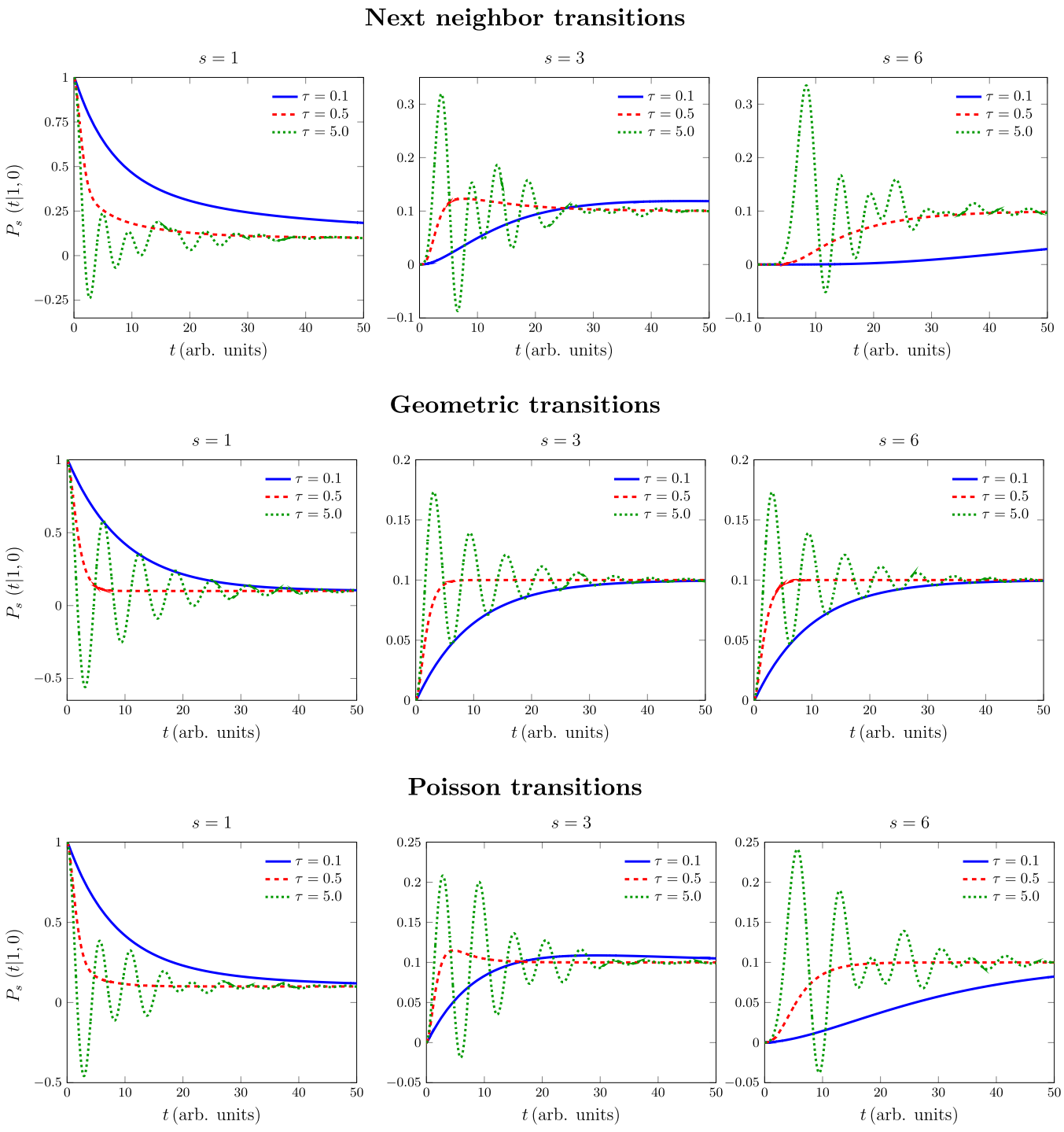

FIG. 1. Probability $P_s(t|s_0 = 1, 0)$ for fixed $\alpha = 1$ and different values of s ($s = 1, 3, 6$) as a function of time t. The plots are for different jump models $\mathbf{T}_{ss'}$ in a ring with $N = 10$ sites. The full blue line corresponds to $\tau = 0.1$ (case $\tau < 1/2\alpha$), the red dashed line corresponds to $\tau = 0.5$ (case $\tau = 1/2\alpha$), and the green dotted line corresponds to $\tau = 5.0$ (case $\tau > 1/2\alpha$), where positivity cannot be assured; see Appendix A for this constraint. The rest of the parameters are $\gamma = 0.5$ (for the geometric jump model) and $\theta = 0.5$ (for the Poisson jump model).

therefore the Fourier transform of $\mathbf{T}_{ss'}$ gives $T(k) = \sum_{s=-\infty}^{\infty} e^{iks}\,\mathbf{T}_{ss'} = \cos(k)$, and so the solution is (15) with the poles:

$$u_{\pm} = \frac{1}{2\tau}[-1 \pm \sqrt{1 - (2\tau\alpha)^2(1 - \cos(k))}]. \qquad (30)$$

4. Transition with a geometrical jump model

In this long-range case, the elements of the transition matrix $\mathbf{T}$ are as follows:

$$\mathbf{T}_{ss'} = \frac{1-\gamma}{2\gamma}(\gamma^{|s-s'|} - \delta_{ss'}), \quad 0 < \gamma < 1, \qquad (31)$$

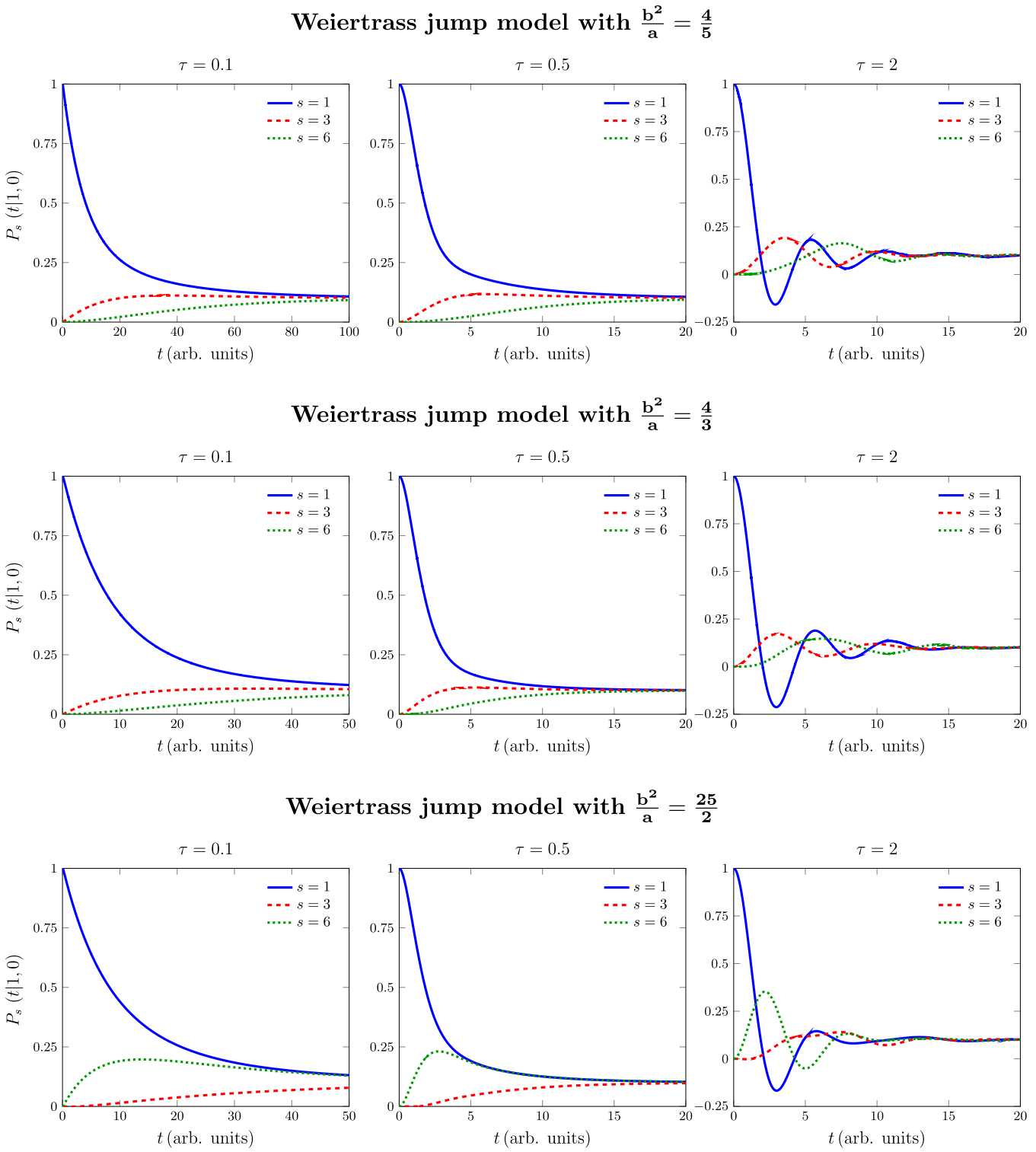

FIG. 2. Probability $P_s(t|s_0 = 1, 0)$ for different values of s ($s = 1, 3, 6$) and fixed $\alpha = 1$, as a function of time t for the Weierstrass jump model in a ring with $N = 10$ sites. The red dashed line corresponds to $s = 3$, the full blue line corresponds to $s = 1$, and the green dotted line corresponds to $s = 6$. The blue line represents s at the IC. The first and the second column correspond to $\tau \leqslant 1/2\alpha$. The third column corresponds to $\tau > 1/2\alpha$ where positivity cannot be assured. The third row corresponds to a case $b^2/a \gg 1$ for the Weierstrass jump model.

and thus its Fourier transform is

$$T(k) = \frac{1-\gamma}{\gamma}\left(\frac{1-\gamma\cos k}{1-2\gamma\cos k+\gamma^2}-1\right). \tag{32}$$

The solution of the lattice TE with geometrical jump transitions is given by (15) with the poles:

$$u_\pm = \frac{1}{2\tau}\left[-1\pm\sqrt{1-(2\tau\alpha)^2\left(1-\frac{1-\gamma}{\gamma}\left(\frac{1-\gamma\cos k}{1-2\gamma\cos k+\gamma^2}-1\right)\right)}\right]. \tag{33}$$

5. Transition with a Poisson jump model

In this case the elements of the transition matrix $\mathbf{T}$ are as follows:

$$\mathbf{T}_{ss'} = \frac{e^{-\theta}}{2(1-e^{-\theta})}\left(\frac{\theta^{|s-s'|}}{|s-s'|!}-\delta_{ss'}\right), \theta>0, \tag{34}$$

and thus its Fourier transform is

$$T(k) = \frac{e^{-\theta}}{2(1-e^{-\theta})}(\exp(\theta e^{ik})+\exp(\theta e^{-ik})-2), \tag{35}$$

and so the solution of the lattice TE with Poisson step transitions is given by (15) with the poles:

$$u_\pm = \frac{1}{2\tau}\left[-1\pm\sqrt{1-(2\tau\alpha)^2\left(1-\frac{e^{-\theta}}{2(1-e^{-\theta})}(\exp(\theta e^{ik})+\exp(\theta e^{-ik})-2)\right)}\right]. \tag{36}$$

6. Transition with a Weierstrass jump model

In this model, there are subclusters within embedded clusters. Then, the elements of the transition matrix $\mathbf{T}$ are

$$\mathbf{T}_{ss'} = \frac{a-1}{2a}\sum_{n=0}^{\infty}\frac{1}{a^n}(\delta_{s-s',b^n}+\delta_{s-s',-b^n}),\ a>1, b\geqslant 1, \tag{37}$$

thus its Fourier transform is

$$T(k) = \frac{a-1}{a}\sum_{n=0}^{\infty}\frac{1}{a^n}\cos(b^n k). \tag{38}$$

Here $1/a^n$ is the probability of making a jump of length b^n. The limit $b\to 1$ corresponds to the usual random-walk model. Futhermore, it can be proved that if $b^2/a>1$, then all moments of the transition probability will diverge [12]. In particular a fractal dimension can be associated with the quantity $\mu = \ln a/\ln b$, [63,71].

The solution of the lattice TE with Weierstrass step transitions is given by (15) with the poles:

$$u_\pm = \frac{1}{2\tau}\left[-1\pm\sqrt{1-(2\tau\alpha)^2\left(1-\frac{a-1}{a}\sum_{n=0}^{\infty}\frac{1}{a^n}\cos(b^n k)\right)}\right]. \tag{39}$$

Remark. Jump models (29), (31), and (34) have in common that all m moments for the transitions are finite:

$$\langle(s-s')^m\rangle = \sum_{s=-\infty}^{\infty}(s-s')^m\,\mathbf{T}_{ss'} = \left[\frac{d^m T(k)}{d(ik)^m}\right]_{k=0} < \infty.$$

However, the Weierstrass jump model has finite moments only if $b^2/a<1$. Therefore, it is important to study the competition of the finite-velocity transport parameters: α,τ [due to the memory kernel in (1)] with the jump parameters. In the limit $t\ll\tau$, the propagator will have a wavelike motion, while in the opposite case, $t\gg\tau$, the propagator will have a diffusive-like motion. However, the crossover and the dynamic coefficients will strongly depend on the structure $T(k)$.

III. SECOND MOMENT ON THE INFINITE LATTICE

We can now calculate the dispersion of the finite-velocity transport for the different jump structures in the free 1D lattice. To perform this evaluation we use the generic solution (15) for different models of jumps in the lattice.

Let us start with the next-nearest-neighbor jump model (29). In this case, $T(k)=\cos k$, therefore introducing the expansion $T(k)\simeq 1-\frac{1}{2}k^2+\mathcal{O}(k^4)$ in the poles (13), and taking the second derivative, we get the second moment for the generalized transport in the infinite lattice. Starting from s_0 at $t_0=0$ we use

$$\langle(s(t)-s_0)^2\rangle = -\left[\frac{d^2}{dk^2}P_k(t)\right]_{k=0}. \tag{40}$$

From this expression we can analyze the short- and long-time regime to obtain the results:

$$\lim_{t\to 0}\langle(s(t)-s_0)^2\rangle \to \frac{\alpha^2}{2}t^2+\cdots, \tag{41}$$

$$\lim_{t\to\infty}\langle(s(t)-s_0)^2\rangle \to \alpha^2\tau t+\alpha^2\tau^2(e^{-t/\tau}-1)+\cdots. \tag{42}$$

These results show the wave and diffusive regimes.

Our second example, is the geometric jump structure (31). In this case, $T(k)$ is given by (32), and we have $T(k)\simeq$

$1-\frac{1}{2}[(1+\gamma)/(\gamma-1)^2]k^2+\mathcal{O}(k^4)$. From this expression, we obtain:

$$\lim_{t\to 0}\langle (s(t)-s_0)^2\rangle \to \frac{\alpha^2(1+\gamma)}{2(\gamma-1)^2}t^2+\cdots, \tag{43}$$

$$\lim_{t\to\infty}\langle (s(t)-s_0)^2\rangle \to \frac{\alpha^2\tau(1+\gamma)}{(\gamma-1)^2}t-\frac{\alpha^2\tau^2(1-e^{-t/\tau})(1+\gamma)}{(\gamma-1)^2}+\cdots. \tag{44}$$

The third example would be the Poisson jump structure (34). In this case, $T(k)$ is given by (35), and $T(k)\simeq 1-\frac{1}{2}[\theta e^\theta(1+\theta)/(e^\theta-1)]k^2+\mathcal{O}(k^4)$. Therefore, introducing $T(k)$ in the poles (13) and taking the second derivative we get the second moment. As before, we get for the short and long time:

$$\lim_{t\to 0}\langle (s(t)-s_0)^2\rangle \to \frac{\alpha^2\theta e^\theta(1+\theta)}{2(e^\theta-1)}t^2+\cdots, \tag{45}$$

$$\lim_{t\to\infty}\langle (s(t)-s_0)^2\rangle \to \frac{\alpha^2\tau e^\theta\theta(1+\theta)}{(e^\theta-1)}t-\frac{\alpha^2\tau^2(1-e^{-t/\tau})e^\theta\theta(1+\theta)}{(e^\theta-1)}\cdots. \tag{46}$$

All of these expressions are for the infinite lattice and show how the crossover from ballistic to linear behavior is dominated by the jumping structure $T(k)$. The effective velocity and the diffusion coefficient depend on the jumping parameters.

A. Effective dynamic coefficients

From the time-dependent second moment it is possible to deduce the behavior of the effective dynamic coefficients. In fact, from (41), (43), and (45) we see that the velocity v is characterized by

$$v^2=\begin{cases}\frac{\alpha^2}{2} & \text{for next-neighbor transitions}\\ \frac{\alpha^2(1+\gamma)}{2(\gamma-1)^2} & \text{for geometric jump transitions}\\ \frac{\alpha^2\theta e^\theta(1+\theta)}{2(e^\theta-1)} & \text{for Poisson jump transitions}\end{cases}. \tag{47}$$

We observe that the larger the jumping probability, the greater the velocity will be.

From the long-time behavior of the second moment, it is also possible to deduce the diffusion coefficient. In fact from (42), (44), and (46) we see that the diffusion coefficient D is characterized by

$$D=\begin{cases}\alpha^2\tau & \text{for next-neighbor transitions}\\ \frac{\alpha^2\tau(1+\gamma)}{(\gamma-1)^2} & \text{for geometric jump transitions}\\ \frac{\alpha^2\tau\theta e^\theta(1+\theta)}{(e^\theta-1)} & \text{for Poisson jump transitions}\end{cases}. \tag{48}$$

As before, the larger the jumping probability is, the larger the diffusion coefficient will be. Another expected result related to the lattice finite-velocity transport approach is that the effective velocity only depends on the timescale α^{-1}, while the diffusion coefficient depends on the group $\alpha^2\tau$. The jumping model affects both coefficients in the same way.

Since the pioneering work of Montroll and Weiss [61], the solution of the random walk in the n-dimensional torus has been introduced to achieve an analytical solution. Additionally, the physical behavior of finite systems is important in experimental situations [62]. Therefore, to study the transport of information towards the completely disordered state, we will now calculate the Shannon entropy. The present lattice approach allows for an exact calculation (a polynomial formula) of the entropy in a ring, which differs from the Shannon entropy in the space-continuous TE [57].

IV. THE FINITE-VELOCITY TRANSPORT APPROACH ON THE RING

A. Generic solution

The ring is a particularly interesting topological domain for studying the properties of finite-velocity transport. A ring with N sites is a model that considers the characteristics of a finite domain in a simple way.

The solution in a ring can be constructed using the method of images [12,62]. Let $P^0(k,t)$ be the solution (in the Fourier representation) on the free 1D domain. Noting that in the ring the conditional probability fulfills $P_s(t|s_0,t_0)=P_{s+N}(t|s_0,t_0)$, we can write [12]

$$P_s(t|s_0,t_0)=\frac{1}{N}\sum_{\nu=1}^{N}\exp\left(-i\frac{2\pi\nu}{N}s\right)P^0\left(k=\frac{2\pi\nu}{N},t-t_0\right). \tag{49}$$

In a finite domain, the Fourier number is quantized. This formula is generic and valid for any transition probability $\mathbf{T}_{ss'}$. Taking $t_0=0$ and $P_k(0)=e^{iks_0}$, from (15) and the poles (13), we get

$$P_s(t|s_0,0)=\frac{1}{N}\sum_{\nu=1}^{N}e^{-i\frac{2\pi\nu}{N}(s-s_0)}\times\left[\frac{1}{\tau}\left(\frac{e^{tu_+}-e^{tu_-}}{u_+-u_-}\right)+\left(\frac{u_+e^{tu_+}-u_-e^{tu_-}}{u_+-u_-}\right)\right]_{k=\frac{2\pi\nu}{N}}. \tag{50}$$

The conditioned q moments in the ring can be calculated as ($q=1,2,3,\ldots$):

$$\langle s(t)^q\rangle_{s_0}=\sum_{s=1}^{N}s^qP_s(t|s_0,0)=\left\{\sum_{\nu=1}^{N}\frac{e^{iks_0}}{N}\left[\frac{1}{\tau}\left(\frac{e^{tu_+}-e^{tu_-}}{u_+-u_-}\right)+\left(\frac{u_+e^{tu_+}-u_-e^{tu_-}}{u_+-u_-}\right)\right]\sum_{s=1}^{N}s^qe^{-iks}\right\}_{k=\frac{2\pi\nu}{N}}. \tag{51}$$

These expressions complete the solution for the finite-velocity transport approach on the ring, for any jump structure $T(k)$ appearing in the poles (13). In the stationary state, these moments $\langle s^q\rangle$ can be readily calculated, so what is interesting is the transient behavior from the IC (we will take $s_0=1$).

B. Probability on the ring for different jump models

Here we present the solution $P_s(t|s_0,0)$, as described in (50) within a ring for different jump models $\mathbf{T}_{ss'}$. It is important to note that through explicit construction detailed in Appendix A, we have proved that in order to ensure a well-posed continuous-time representation of a Markov chain $\mathbf{T}^n \to \mathbf{W}(t)$, it is necessary to fulfill the constraint $\tau < 1/2\alpha$ to assure the application of the renewal theory.

As posited by Bochner's theorem, in order to assure the positivity of the solution, we should prove the concavity of the characteristic function $P_k(t)$ from (15), which is a formidable task for arbitrary structure function $T(k)$. However, we have proved in Appendix A for arbitrary $T(k)$ that if $\tau < 1/2\alpha$, then the solution will be positive. The inverse is more complicated: If $\tau > 1/2\alpha$, then we have shown numerically that a negative value $P_s(t|s_0,0)$ for some instant of time t can appear. The appropriate value of τ depends on the jump structure $T(k)$. This behavior will be illustrated in Fig. 1 for some cases.

First, let us start by analyzing the regular next-nearest-neighbor jump model. In this case, the poles are characterized by the structure (30). The geometrical and Poisson jump models can readily be written using the poles given by (32) and (35), respectively. In Fig. 1, we have shown $P_s(t|s_0 = 1, t = 0)$ for different sites $s = \{1, 3, 6\}$ in a ring with $N = 10$ sites, for fixed $\alpha = 1$ and different timescales τ. For cases: (a) regular next-nearest-neighbor, (b) geometrical, and (c) Poisson jump model. Therefore, the following timescale regimes can be appreciated: $\tau < 1/2\alpha$, $2\alpha\tau = 1$, and $\tau > 1/2\alpha$. We remind that the critical value $\tau = 1/2\alpha$ characterizes the transition to the wavelike behavior. The probability to be at sites $s > s_0$ clearly depends on time, and the convergence to the stationary state [fully disordered state: $P_s(t \to \infty|s_0,0) \to 1/N$] is monotonous in time for $\tau < 1/2\alpha$, and is faster for jump models with long-range transition probabilities, as in the geometrical jump model. As commented before, for each $T(k)$, different behavior occurs for $2\alpha\tau > 1$, where a wavy-like regime can be seen for $\tau = 5.0$ with $\alpha = 1$. In the same figure we noted that for a fixed α and large-enough τ, the wavy solution $P_s(t|s_0,0)$ can become negative for some t. Depending on $T(k)$, the value of time t when $P_s(t|s_0,0) < 0$ can be observed, even for the next-nearest-neighbor jump model.

Now we will show the solution $P_s(t|s_0,0)$ using the Weierstrass jump model characterized by the poles (39). As pointed out before, this model becomes particularly anomalous if $b^2/a > 1$, since in this scenario, within an infinite lattice, all jump moments would diverge. In Fig. 2, we can compare the solution $P_s(t|s_0,0)$ for different sites s in a ring with $N = 10$ for fixed $\alpha = 1$ as a function of time t and for different values of τ. A particularly notable result from the Weierstrass jump model is that if $b^2/a \gg 1$, then sites that are far away from the initial condition are populated faster than the nearest-neighbor sites from s_0.

V. SHANNON ENTROPY FOR THE LATTICE TE ON THE RING

The Shannon entropy is a number assigned to a partition set, $S = -\langle \ln P \rangle$. This is simple if the random variable is of the discrete type. In the present work, we are interested in the time-dependent evolution of the probability assigned to each site s in a ring with N sites. This evolution has been characterized by a generalized finite-velocity ME transport. Therefore, the partition set will be associated with the time-dependent probability assigned to each site in the ring from a given initial condition $P_s(t \to 0|s_0,0) \to \delta_{s,s_0}$. We have found the solution for a generic transition probability $\mathbf{T}_{ss'}$ in the ring, and it is characterized by the poles (13). Thus, we can write the time-dependent Shannon's entropy:

$$S(t) = -\sum_{s=1}^{N} P_s(t|s_0,0) \ln P_s(t|s_0,0), \tag{52}$$

where $P_s(t|s_0,0)$ is written, in (50), in terms of any structure jump model $\mathbf{T}(k)$.

Due to the fact that the stationary solution in the ring is equally distributed in the partition set, we obtain $P_s(t \to \infty|s_0,0) \to 1/N$. Then the entropy will reach its maximum value $S(t \to \infty) \to \ln N$. Thus, it is important for the characterization of the transport of information to study the relaxation to this stationary value as a function of the timescales $\{\tau, \alpha^{-1}\}$, and the parameters of the jump model $T(k)$. As can be seen from (50), as $t \to \infty$ the approach to the entropic disordered state is controlled by the behavior of the poles $u_\pm(k)$.

Interestingly, the transport of information in the process can be better studied from the time variation of the Shannon entropy. Therefore, we will be interested in the time derivative of Shannon's entropy,

$$\begin{aligned}\frac{dS(t)}{dt} &= -\frac{d}{dt}\sum_{s=1}^{N} P_s(t|s_0,0) \ln P_s(t|s_0,0) \\ &= -\sum_{s=1}^{N} \dot{P}_s(t|s_0,0) \ln P_s(t|s_0,0),\end{aligned} \tag{53}$$

where $\dot{P}_s(t|s_0,0)$ can readily be obtained by taking the time derivative in (50).

Let us now analyze the time variation $dS(t)/dt \equiv \dot{S}(t)$ in the regime $2\alpha\tau < 1$. From this analysis, it can be appreciated that the entropy variation has a maximum that depends in a nontrivial way on the jump parameters and timescales $\{\tau, \alpha^{-1}\}$ [in this case, the velocity $\dot{S}(t)$ is always positive]. If $2\alpha\tau > 1$, then it is possible that $\dot{S}(t)$ can decrease even more and turn to be negative, so at a certain time t, the entropy $S(t)$ (not for the case $\tau = 1.0$ in Fig. 3) is not defined because $P_s(t|s_0,0)$ becomes negative (as occurs in some cases in Figs. 1 and 2). This situation strongly depends on the model of the jump $\mathbf{T}_{ss'}$ under the necessary condition $2\alpha\tau > 1$.

In Fig. 3, we have plotted the entropy velocity $\dot{S}(t)$ as a function of time t for fixed $\alpha = 1$, for two values of τ and different jump structures $T(k)$, in all cases the IC is $s_0 = 1$. For $\tau = 0.1$ (corresponding to $\tau < 1/2\alpha$) in all cases (next-nearest-neighbor, geometrical, Poisson, and Weierstrass jump models), $\dot{S}(t)$ is a single-peak function with a monotonically decreasing behavior as a function of time t. For $\tau = 1.0$ and 0.8 (corresponding to $\tau > 1/2\alpha$) $\dot{S}(t)$ shows a nonmonotonic behavior as a function of time t. Nevertheless, these

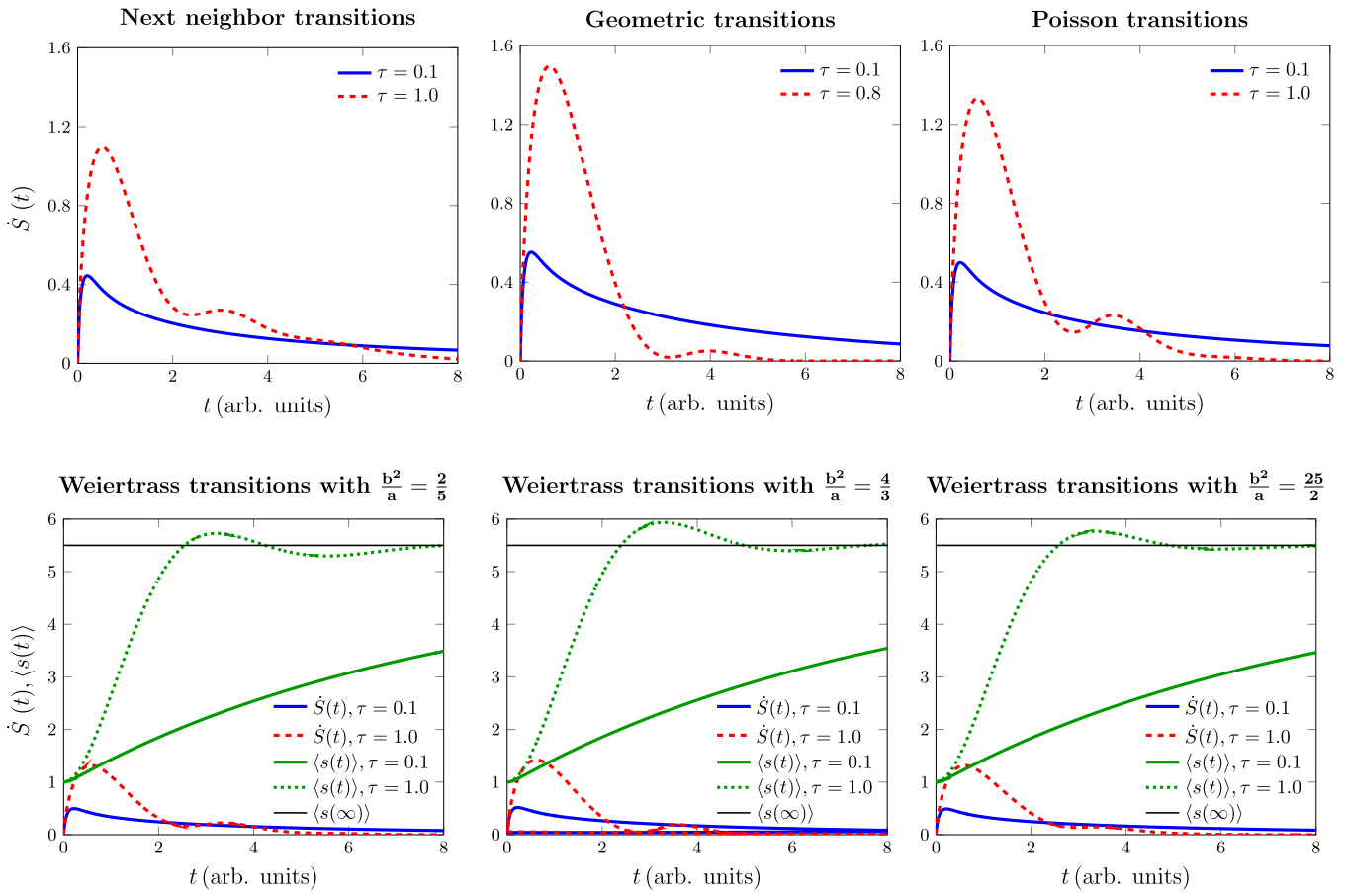

FIG. 3. The entropy velocity $dS(t)/dt$ for fixed $\alpha = 1$ is shown as a function of time t for the regular next-nearest-neighbor, geometrical, Poisson, and Weierstrass jump models in a ring with $N = 10$ sites. The entropy is always well defined (positive) if $\tau < 1/2\alpha$. Nevertheless, here we show in a red dashed line cases corresponding to $\tau = 1.0$ (0.8 for the geometric case) corresponding to $\tau > 1/2\alpha$. The full blue line corresponds to $dS(t)/dt$ for $\tau = 0.1$ (corresponding to $\tau < 1/2\alpha$). The red dashed line represents $dS(t)/dt$ for a value of $\tau > 1/2\alpha$, but the parameters were chosen such that wavylike motion always fulfills $P_s(t|s_0, 0) > 0$. The first moment associated with the Weierstrass jump model with $\tau = 1.0$ and $\tau = 0.1$ are shown in green dotted lines and full lines, respectively, for the different values of the rate b^2/a to compare with the behavior of $dS(t)/dt$.

parameters have been chosen to correspond to a (positive) wavylike transport motion.

In the Weierstrass jump model, $\dot{S}(t)$ is shown in the same figure for different values of the rate b^2/a ($\lesssim 1$ and $\gg 1$). We remind that due to the finite domain of the ring, the moments of $P_s(t|s_0, 0)$, which can readily be obtained from (51), are finite. This is a difference from the calculation in an infinite lattice (40). For the Weierstrass jump model the behavior of the first moment, $\langle s(t)\rangle_{s_0}$, is shown in the figure for different τ and rate b^2/a. There the asymptotic value can be checked as $\langle s(t \to \infty)\rangle_{s_0} \to (1 + N)/2$. We note that in the limit as b approaches 1, for any value of a, the Weierstrass jump model converges to the next-nearest-neighbor model. In Fig. 4 we show the comparison of $\dot{S}(t)$ against the second moment $\langle s^2(t)\rangle_{s_0}$, the main peak in the entropy velocity shows the transition from ballistic to diffusive behavior. The second moment associated with the cases $\tau > 1/2\alpha$ show a wavy behavior, but in any case, the asymptotic value is $\langle s^2(t \to \infty)\rangle \to (1 + 3N + 2N^2)/6$.

Alternatively, using the equation $\ddot{P}_s(t|s_0, 0) + \dot{P}_s(t|s_0, 0)/\tau = \alpha^2 \sum_s \mathbf{H}_{ss'} P_{s'}(t|s_0, 0)$, we can express the time variation with respect to the ordinary diffusive case as:

$$\Delta\dot{S}(t) = \tau \sum_{s=1}^{N} \ddot{P}_s(t|s_0, 0) \ln P_s(t|s_0, 0), \tag{54}$$

with $P_s(t|s_0, 0)$ given by (50) and $\ddot{P}_s(t|s_0, 0)$ by the expression:

$$\ddot{P}_s(t|s_0, 0) = \frac{1}{N} \sum_{\nu=1}^{N} e^{-i\frac{2\pi\nu}{N}(s-s_0)} \left[\frac{1}{\tau} \left(\frac{u_+^2 e^{tu_+} - u_-^2 e^{tu_-}}{u_+ - u_-} \right) + \left(\frac{u_+^3 e^{tu_+} - u_-^3 e^{tu_-}}{u_+ - u_-} \right) \right]_{k=\frac{2\pi\nu}{N}}, \tag{55}$$

where $u_\pm \equiv u_\pm(k)$ are given by (13) for any jumping model characterized by $T(k)$. From (54), we see that in the limit $\tau \to 0$ with $\alpha \to \infty$ such that $\tau\alpha^2 \to \lambda$, we arrive at $\Delta\dot{S}(t) = 0$.

VI. CONCLUSIONS

Starting with a non-local-in-time master equation, we have studied a generic finite-velocity transport approach on the lattice and specifically solved the generalized telegrapher's

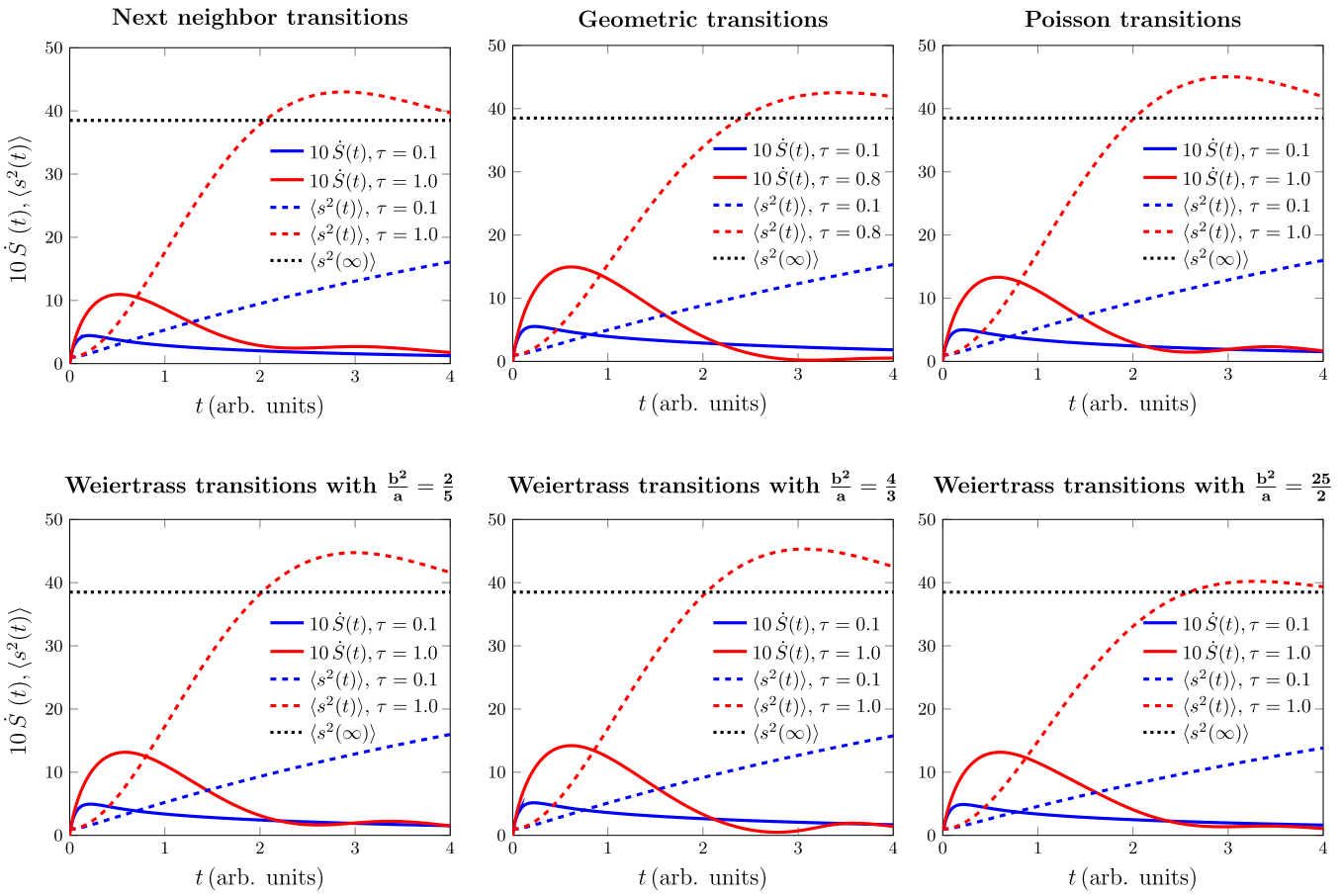

FIG. 4. The entropy velocity $10 \times dS(t)/dt$ (full lines) for fixed $\alpha = 1$ is shown as a function of time t for the regular next-nearest-neighbor, geometrical, Poisson, and Weierstrass jump models in a ring with $N = 10$ sites. Dashed lines correspond to the second moment $\langle s^2(t)\rangle$ for different values of τ to be compared with the change in the behavior of $dS(t)/dt$. The blue line corresponds to $\tau < 1/2\alpha$, the red line corresponds to $\tau > 1/2\alpha$, but the parameters were chosen such that wavylike motion is always positive. The black dotted line represents the point reached by $\langle s^2(t)\rangle$ after a long time.

equation on the ring. Several transition matrices have been used to characterize different jump structures $\mathbf{T}_{ss'}$ on the lattice. Specifically, we have solved the probability distribution with (a) regular next-nearest-neighbor jump, (b) geometrical jump, (c) Poisson jump, and (d) Weierstrass jump, all these cases for timescales $\tau \leqslant 1/2\alpha$ and $\tau > 1/2\alpha$. By construction, we have proved that if $\tau < 1/2\alpha$, then the solution $\mathbf{W}(t)$ is positive because a waiting-time function from renewal theory exists. In the reverse case $\tau > 1/2\alpha$, the kernel is not completely monotonous; therefore, following Feller's theorem, the existence of a positive waiting-time density $\psi(t)$ cannot be assured, see Appendix A. A different task is to prove from the characteristic function (15) the positivity of the inverse; in this case, Bochner's theorem should be used, but this is out of the scope of the present paper.

The second moment on the infinite lattice has been calculated analytically for different jumping structures $T(k)$; therefore effective transport coefficients have been defined, see (47) and (48). In addition, we have calculated analytically the solution of the time-dependent probability for the finite-velocity transport approach on a ring with N sites. The Shannon entropy is also calculated analytically as a polynomial, which is an advantage when compared with the continuous model that does not have an analytical expression [57]. The transition to its maximum value $S(t \to \infty) \to \ln N$ in the (fully disordered) stationary state has been studied as a function of the timescales α^{-1} and τ, as well as a function of the parameters characterizing different hopping models $\mathbf{T}_{ss'}$. The entropy velocity $\dot{S}(t)$ has been plotted as a function of the physical parameter. It is concluded that there is a maximum for this velocity that depends on the timescales α^{-1}, τ, and the parameters of the jump structure, see (31), (34), and (37). This maximum shows the ballistic to diffusive transition. The higher the probability for long-range hopping, the faster the information is moved to sites far away from the initial condition. This is particularly notable when observing how the population far apart from site s_0 is anticipated with respect to sites $s \gtrsim s_0$ for the Weierstrass jump model when $b^2/a \gg 1$, as shown in Fig. 2. The time behavior of $\dot{S}(t)$ has also been compared with the behavior of the first and second moments in the ring conditioned to the IC $P_s(t \to 0|s_0, 0) \to \delta_{ss_0}$, showing that the transport of information can be associated with $\dot{S}(t)$ (see Figs. 3 and 4). The study of Shannon entropy in a ring is an interesting objective, and its relevance lies in

addressing the transport of information in finite systems with applications in solid-state physics and biophysics [62,63].

In this work, we have been interested in the case when $\tau < 1/2\alpha$. However, we have shown that for $\tau > 1/2\alpha$, the solution $P_s(t|s_0, 0)$ can become negative at some time t depending on the structure $T(k)$. Of particular interest is the study of dissipative waves in disordered lattices; this is the case to be analyzed in future contributions.

In Appendix B, we have presented the nonhomogeneous TE in the continuous limit. New interesting results concerning the initial condition $\dot{P}_s(0) \neq 0$ on the non-local-in-time ME (1) can be worked out in the context of a nonhomogeneous lattice TE. This subject is in progress.

APPENDIX A: ON THE MEMORY KERNEL $\Phi(t)$ AND THE RENEWAL APPROACH

To interpret the parameters $\{\alpha, \tau\}$ from a diffusive-like point of view, we propose the following analysis. We have noted before that $\Phi(t)$ can be associated with a renewal probability theory [69], in fact, this is so only if the parameters of the kernel fulfill the condition:

$$\tau < \frac{1}{2\alpha}. \tag{A1}$$

This restriction can be interpreted by defining a waiting-time probability density function $\psi(t)$ applied to the Markov chain:

$$\mathbf{T}(m + m') = \mathbf{T}(m) \cdot \mathbf{T}(m'), \ \{m, m'\} \in 0, 1, 2, \cdots, \tag{A2}$$

with m, m' positive discrete time indices.

The continuous-time representation of a discrete-time Markov chain can be incorporated by using the renewal approach [61]. We consider a 1D lattice with translational invariance; thus, let $\varphi(t)$ be the probability of remaining at any site s without jumping during the interval of time $[0, t]$

$$\varphi(t) = 1 - \int_0^t \psi(t')dt'. \tag{A3}$$

This equation defines the waiting-time function $\psi(t)$ between successive jumps in the Markov chain. Therefore, the mean waiting time is

$$\langle t \rangle = \int_0^\infty t\psi(t)dt.$$

Introducing the notation for the Laplace transform:

$$\varphi(u) \equiv \mathcal{L}[\varphi(t)] = \int_0^\infty \varphi(t)e^{-ut}dt, \ \psi(u) \equiv \mathcal{L}[\psi(t)], \text{ etc.},$$

and using the Green function of (1), we can prove the relation (see below):

$$\Phi(u) = \frac{u\psi(u)}{1 - \psi(u)}. \tag{A4}$$

From this equation, it is simple to see that only if the waiting time $\psi(t)$ is an exponential function, then the kernel $\Phi(t)$ will be a Dirac-delta function, restoring a Markovian character in the continuous-time representation of $\mathbf{T}(m)$.

Conversely, equation (A4) can be used to solve $\psi(u)$ in the form

$$\psi(u) = \frac{\Phi(u)}{u + \Phi(u)}. \tag{A5}$$

Then, from the exponential memory kernel (4), in the Laplace representation we obtain:

$$\psi(u) = \frac{\alpha^2}{\alpha^2 + u(u + 1/\tau)},$$
$$\text{thus } \langle t \rangle = -\left.\frac{d\psi(u)}{du}\right|_{u=0} = \frac{1}{\alpha^2\tau}. \tag{A6}$$

In addition, from the inverse Laplace transform of $\psi(u)$, we arrive at the waiting-time probability density in real-time representation:

$$\psi(t) = \frac{2\tau\alpha^2 e^{-t/2\tau}}{\sqrt{1 - (2\alpha\tau)^2}} \sinh\left(\frac{t}{2\tau}\sqrt{1 - (2\alpha\tau)^2}\right),$$
$$\int_0^\infty \psi(t)dt = 1. \tag{A7}$$

In order to obtain a positively normalized density $\psi(t)$, we need to satisfy condition (A1). Therefore, the diffusion-like restriction (A1), can be interpreted as the condition that the flight time α^{-1} is smaller than the mean waiting time $\langle t \rangle = (\alpha^2\tau)^{-1}$.

In summary, by construction for any $T(k)$ and using renewal theory, the positivity of the continuous-time solution is assured if (A1) is fulfilled. For the case $\tau > 1/2\alpha$, the positivity depends on the specific hopping structure function $T(k)$, and its proof depends on the concavity of the characteristic function (15); that is, to fulfill Bochner's theorem.

1. Proof of (A4)

Consider the discrete-time Markov chain (A2) where $\mathbf{T}(m)$ is the evolution of the Markov chain at discrete time m with $\mathbf{T}$ as a generic transition matrix with elements that fulfill:

$$\mathbf{T}_{ss'} \geqslant 0, \forall\{s, s'\} \in \mathcal{D}_s \quad \text{and} \quad \sum_{s\in\mathcal{D}_s} \mathbf{T}_{ss'} = 1, \forall s' \in \mathcal{D}_s. \tag{A8}$$

The solution of (A2) is as follows:

$$\mathbf{T}(n) = \mathbf{T} \cdot \mathbf{T}^{n-1}. \tag{A9}$$

Using the renewal approach, the continuous-time representation can be written in the form [61]:

$$\mathbf{W}(t) = \sum_{n=1}^\infty \mathcal{P}_n(t)\mathbf{T}^n + \left(1 - \int_0^t \psi(t')dt'\right)\mathbf{T}(0), \tag{A10}$$

where $\mathbf{T}(0) = \mathbf{1}$ (identity), and we have assumed synchronization for the first waiting-time function [68]; that is, $\psi_1(t) = \psi(t)$. For a stationary renewal process, $\mathcal{P}_n(t)$ is the probability of having n events in the time interval $[0, t]$, which can be written, in the Laplace representation, as:

$$\mathcal{P}_n(u) = \int_0^\infty e^{-ut}\mathcal{P}_n(t)dt = \frac{1 - \psi(u)}{u}\psi(u)^n. \tag{A11}$$

Here $\psi(t)$ is a generic waiting-time probability density function characterizing the renewal process. A general presentation considering $\psi_1(t) \neq \psi(t)$ can be seen in Ref. [72].

The continuous-time version of the chain evolution (A9) at discrete time n is represented by (A10) as an infinite sum of possible ways to arrive at a particular site s at continuous time t, considering all waiting times in previous sites s' coming from the initial condition s_0; that is, the conditional probability (matrix elements) $\mathbf{W}(t)_{s,s_0}$. This is what is now called, in modern jargon, the CTRW approach to characterize non-Markov random-walk processes [62].

In the Laplace representation, the solution of (A10) is as follows:

$$\mathbf{W}(u) = \frac{1-\psi(u)}{u}(1-\psi(u)\mathbf{T})^{-1}. \tag{A12}$$

Thus, the evolution equation of the continuous-time probability matrix $\mathbf{W}(u)$ can be written in the Laplace representation as:

$$\begin{aligned} u\mathbf{W}(u) - \mathbf{1} &= u\frac{1-\psi(u)}{u(1-\psi(u)\mathbf{T})} - \mathbf{1} = \frac{\psi(u)(-\mathbf{1}+\mathbf{T})}{(1-\psi(u)\mathbf{T})} \\ &= \frac{u\psi(u)}{(1-\psi(u))}(\mathbf{T}-\mathbf{1})\mathbf{W}(u). \end{aligned} \tag{A13}$$

In this formula we have used the initial condition for the Green function $\mathbf{W}(0) = \mathbf{1}$. Therefore, Eq. (A13) can be compared with the Green function of (1). In fact, this equation can be written in the real-time representation as a non-local-in-time ME:

$$\partial_t \mathbf{W}(t) = \int_0^t \Phi(t-t')(\mathbf{T}-\mathbf{1})\mathbf{W}(t')dt',$$

where the kernel $\Phi(u)$ is the one presented in (A4). That is, any positive and normalized waiting-time function $\psi(t)$ characterizes a particular kernel $\Phi(t)$.

We note that the reverse is not true; there can be a kernel that is not associated with a positive and normalized waiting time. This is the case of the kernel (4) when (A1) is not fulfilled, because in this case $\Phi(u)$ is not a completely monotone function. See Feller's theorem 1 (p. 439) in Ref. [68].

APPENDIX B: THE CONTINUOUS TE

1. The ordinary TE

In the continuous limit, the ME operator transforms into a second-order space derivative (27). Then, in the limit $\epsilon \to 0$, $\alpha \to \infty$ such that $\frac{1}{2}(\epsilon\alpha)^2 \to v^2$, we can define a velocity. Using (1) we arrive at

$$\partial_t P(x,t) = v^2 \int_0^t e^{-(t-t')/\tau}\, \partial_x^2 P(x,t')\, dt'. \tag{B1}$$

The initial condition $\partial_t P(x,t)|_{t=0} = 0$ is implicit in (B1). Taking the time derivative of this equation, we get the ordinary TE (hyperbolic diffusion equation):

$$\left[\partial_t^2 + \frac{1}{\tau}\partial_t - v^2\partial_x^2\right]P(x,t) = 0. \tag{B2}$$

2. The nonhomogeneous TE

Nevertheless, if we do not want to keep the zero initial condition, $\partial_t P_s(t)|_{t=0} = 0$ appearing in (B1), then we have to work out a non-local-in-time ME of the form:

$$\partial_t P_s(t) = \alpha^2 \int_0^t e^{-(t-t')/\tau} \sum_{s'\in\mathcal{D}_s} \mathbf{H}_{ss'} P_{s'}(t')\, dt' + \dot{P}_s(0), \tag{B3}$$

where the initial condition appearing in the right-hand side of (B3), $\dot{P}_s(0)$, must be consistent with the IC of the process before the elimination of variables producing the memory kernel in (B3). Then, passing to the continuous limit, we obtain:

$$\partial_t P(x,t) = v^2 \int_0^t e^{-(t-t')/\tau}\, \partial_x^2 P(x,t')\, dt' + \dot{P}(x,0). \tag{B4}$$

As before, taking the time derivative in (B4) we obtain:

$$\left[\partial_t^2 + \frac{1}{\tau}\partial_t - v^2\partial_x^2\right]P(x,t) = \frac{\dot{P}(x,0)}{\tau}. \tag{B5}$$

This nonhomogeneous equation has a flux term $\dot{P}(x,0)/\tau$ when compared with the ordinary TE (B2). This equation is useful when we are interested in working with a "bullet" initial condition. For example, in the form:

$$\begin{aligned} P(x,t)|_{t=0} &= \delta(x-vt)|_{t=0}, \\ \partial_t P(x,t)|_{t=0} &= -v\delta'(x-vt)|_{t=0}. \end{aligned} \tag{B6}$$

In the context of finite-velocity diffusion problems, this IC is quite useful to describe transport with an incoming flux in the domain of interest. The general solution of this nonhomogeneous hyperbolic diffusion equation can be obtained by introducing the Fourier-Laplace transform.

a. Solution of the nonhomogeneous TE (B5)

To solve (B5) we introduce the continuous Fourier and Laplace transforms:

$$P(k,u) = \int_{-\infty}^{\infty} dx\, e^{ikx} \int_0^{\infty} dt\, e^{-ut}\, P(x,t) \tag{B7}$$

in (B5), using the IC:

$$P(k,t)|_{t=0} \equiv P(k,0) \text{ and } \partial_t P(k,t)|_{t=0} \equiv \dot{P}(k,0).$$

Then, we obtain

$$P(k,u) = \frac{P(k,0) + \tau\dot{P}(k,0)[1+(\tau u)^{-1}]/(\tau u+1)}{u + \tau v^2 k^2/(\tau u+1)}. \tag{B8}$$

It can be seen that the nonhomogeneous term in (B4) leads to an extra contribution proportional to $\dot{P}(k,0)$ in the RHD of (B8). That is, the term $\tau\dot{P}(k,0)(\tau u)^{-1}/(\tau u+1)$, which has a profound difference when compared with the solution of the ordinary TE.

From the solution (B8) we can study both limits $\tau u \gg 1$ (wave motion at short times) and $\tau u \ll 1$ (diffusion at long times).

b. Short times

Taking the limit $\tau u \gg 1$ in (B8) we arrive to

$$P(k,u) = \frac{P(k,0) + \tau \dot{P}(k,0)[1 + (\tau u)^{-1}]/(\tau u + 1)}{u + \tau v^2 k^2/(\tau u + 1)} \sim \frac{P(k,0) + \tau \dot{P}(k,0)/\tau u}{u + \tau v^2 k^2/\tau u} = \frac{uP(k,0) + \dot{P}(k,0)}{u^2 + v^2 k^2}. \tag{B9}$$

This solution provides a generic wavelike motion at short times.

c. Long times

Taking the limit $\tau u \ll 1$ in (B8) we arrive to

$$P(k,u) = \frac{P(k,0) + \tau \dot{P}(k,0)[1 + (\tau u)^{-1}]/(\tau u + 1)}{u + \tau v^2 k^2/(\tau u + 1)} \sim \frac{P(k,0) + \tau \dot{P}(k,0)(\tau u)^{-1}}{u + \tau v^2 k^2} = \frac{P(k,0) + \dot{P}(k,0)/u}{u + \tau v^2 k^2}. \tag{B10}$$

This solution provides diffusion-like motion at long times, with an incoming flux.

[1] W. Thomson, On the theory of the electric telegraph, Proc. R. Soc. Lond. Ser. I **7**, 382 (1854).

[2] J. M. Pearson, *A Theory of Waves* (Allyn & Bacon, Boston, 1966).

[3] L. D. Landau, J. S. Bell, and M. J. Kearsley, in *Electrodynamics of Continuous Media* (Elsevier Science, Amsterdam, 2013).

[4] E. Argence and T. Kahan, in *Theory of Waveguides and Cavity Resonators* (Hart, New York, 1968).

[5] O. Heaviside, *Electrical Papers of Oliver Heaviside* (Chelsea, New York, 1970), Vol. 1.

[6] C. Cattaneo, Sulla conduzione del calore, Atti Sem. Mat. Fis. Univ. Modena **3**, 83 (1948).

[7] Casas-Vazquez, D. Jou, and G. Lebon, *Extended Irreversible Thermodynamics* (Springer, Berlin, 1996).

[8] N. G. van Kampen, A model for relativistic heat transport, Physica **46**, 315 (1970).

[9] S. Goldstein, On diffusion by discontinuos movements and on the telegraph equation, Q. J. Mech. Appl. Math. **4**, 129 (1951).

[10] R. Fürth, Einige untersuchungen über brownsche bewegungen an einem einzelteilchen, Annal. Phys. **358**, 177 (1917).

[11] J. Masoliver and K. Lindenberg, Countinuous time persistent random walk: A review and some generalizations, Eur. Phys. J. B **90**, 107 (2017).

[12] M. O. Cáceres, *Non-equilibrium Statistical Physics with Application to Disordered Systems* (Springer, Berlin, 2017).

[13] M. Kac, A stochastic model related to the telegrapher's equation, Rocky Mount. J. Math. **4**, 497 (1974).

[14] P. M. Morse and H. Feshbach, *Method of Theoretical Physics* (Mc Graw–Hill, New York, 1953).

[15] J. Masoliver and G. H. Weiss, Finite-velocity diffusion, Eur. J. Phys. **17**, 190 (1996).

[16] D. Poljak, D. Cavka, and F. Rachidi, Generalized telegrapher's equations for buried curved wires, in *2018 2nd URSI Atlantic Radio Science Meeting (at RASC)* (IEEE, Los Alamitos, CA, 2018).

[17] P. Baccarelli, F. Frezza, P. Simeoni and N. Tedeschi, An analytical study of electromagnetic Deep penetration conditions and implications in lossy media through inhomogeneous waves, Materials **11**, 1595 (2018).

[18] M. O. Cáceres, Finite-velocity diffusion in random media, J. Stat. Phys. **179**, 729 (2020).

[19] T. Sandev, L. Kocarev, R. Metzler, and A. Chechkin, Stochastic dynamics with multiplicative dichotomic noise: Heterogeneous telegrapher's equation, anomalous crossovers and resetting, Chaos Solitons & Fractals **165**, 112878 (2022).

[20] K. Górska, A. Horzela, E. K. Lenzi, G. Pagnini and T. Sandev, Generalized Cattaneo (telegrapher's) equations in modeling anomalous diffusion phenomena, Phys. Rev. E **102**, 022128 (2020).

[21] P. Puri and P. K. Kythe, Discontinuities in velocity gradients and temperature in the Stokes' first problem with non-classical heat conduction, Quart. Appl. Math. **55**, 167 (1997).

[22] E. Marín, On thermal waves, Eur. J. Phys. **34**, L83 (2013).

[23] D. D. Joseph and L. Preziosi, Heat waves, Rev. Mod. Phys. **61**, 41 (1989).

[24] B. Straughan, Oscillatory convection and the Cattaneo law of heat conduction, Ricerche Mat. **58**, 157 (2009).

[25] G. B. Nagy, O. E. Ortiz, and O. A. Reula, The behavior of hyperbolic heat equations' solutions near their parabolic limits, J. Math. Phys. **35**, 4334 (1994).

[26] M. A. Aziz and S. Gavin, Causal diffusion and the survival of charge fluctuations in nuclear collisions, Phys. Rev. C **70**, 034905 (2004).

[27] E. Sonnenschein, I. Rutkevich, and D. Censor, Wave packets and group velocity in absorbing media: Solutions of the telegrapher's equation, Progree Electro. Res. (PIER) **27**, 129 (2000).

[28] D. Zhang and M. Ostoja-Starzewski, Telegraph equation: Two types of harmonic waves, a discontinuity wave, and a spectral finite element, Acta Mech. **230**, 1725 (2019).

[29] M. O. Cáceres, Localization of plane waves in the stochastic telegrapher's equation, Phys. Rev. E **105**, 014110 (2022).

[30] M. Nizama and M. O. Cáceres, Penetration of waves in global stochastic conducting media, Phys. Rev. E **107**, 054107 (2023).

[31] R. Geroch, Relativistic theories of dissipative fluids, J. Math. Phys. **36**, 4226 (1995).

[32] J. Dunkel and P. Hänggi, Relativistic Brownian motion, Phys. Rep. **471**, 73 (2009).

[33] B. Gaveau, T. Jacobson, M. Kac, and L. S. Schulman, Relativistic extension of the analogy between quantum mechanics and Brownian motion, Phys. Rev. Lett. **53**, 419 (1984).

[34] M. Zakari and D. Jou, Equations of state and transport equations in viscous cosmological models, Phys. Rev. D **48**, 1597 (1993).

[35] P. Broadbridge, A. D. Kolesnik, N. Leonenko, and A. Olenko, Random spherical hyperbolic diffusion, J. Stat. Phys. **177**, 889 (2019).

[36] R. Bourret, Turbulent diffusion in two and three dimensions by the random-walk model with memory, Can. J. Phys. **39**, 133 (1961).
[37] P. H. Roberts, On Bourret's hypothesis concerning turbulent diffusion, Can. J. Phys. **39**, 1291 (1961).
[38] R. M. Velasco and L. S. G. Colin, The kinetic foundation of extended irreversible thermodynamics revisited, Phys. Rev. A **44**, 4961 (1991).
[39] J. Jansky and V. P. Pasko, Effect of conductivity perturbations in time-dependent global electric circuit model, J. Geoph. Research: Space Physics **120**, 10,654 (2015).
[40] M. O. Cáceres, Surface gravity waves on randomly irregular floor and the telegrapher's equation, AIP Adv. **11**, 045218 (2021).
[41] M. O. Cáceres, Gravity waves on a random bottom: Exact dispersion-relation, Waves in Random and Complex Media **34**, 734 (2021).
[42] F. Ureña, L. Gavete, J. J. Benito, A. García, and A. M. Vargas, Solving the telegraph equation in 2-D and 3-D using generalized finite difference method (GFDM), Engineering Analysis with Boundary Elements **112**, 13 (2020).
[43] H. S. Wio and M. O. Cáceres, Treatment of scattering anisotropy in neutron diffusion through a random-walk scheme, Ann. Nucl. Energy **12**, 263 (1985).
[44] S. I. Heizler, Asymptotic telegrapher's equation (P1) approximation for the transport equation, Nucl. Sci. Eng. **166**, 17 (2010).
[45] B. Zhang, W. Yu, and M. Mascagni, Revisiting Kac's method: A Monte Carlo algorithm for solving the Telegrapher's equations, Math. Comput. Simul. **156**, 178 (2019).
[46] Y. Shlepnev, Coupled 2D Telegrapher's equations for PDN analysis, in *Proceedings of the IEEE 21st Conference on Electrical Performance of Electronic Packaging and Systems* (IEEE, Los Alamitos, CA, 2012), pp. 171–174.
[47] M. O. Cáceres and H. S. Wio, Non-Markovian diffusion-like equation for transport processes with anisotropic scattering, Physica A **142**563 (1987).
[48] M. O. Cáceres and M. Nizama, Stochastic telegrapher's approach for solving the random Boltzmann-Lorentz gas, Phys. Rev. E **105**, 044131 (2022).
[49] P. Borys, Z. J. Grzywna, and J. Łuczka, Hyperbolic diffusion in chaotic systems, Eur. Phys. J. B **83**, 223 (2011).
[50] M. O. Cáceres, Coupled generalized master equations for Brownian motion anisotropically scattered, Phys. Rev. A **33**, 647 (1986).
[51] M. Giona, A. Cairoli, and R. Klages, Extended poisson-kac theory: A unifying framework for stochastic processes with finite propagation velocity, Phys. Rev. X **12**, 021004 (2022).
[52] K. Martens, L. Angelani, R. Di Leonardo, and L. Bocquet, Probability distributions for the run-and-tumble bacterial dynamics: An analogy to the Lorentz model, Eur. Phys. J. E **35**, 84 (2012).
[53] K. H. Pettersen and G. T. Einevoll, Neurophysics: What the telegrapher's equation has taught us about the brain, in *An Anthology of Developments in Clinical Engineering and Bioimpedance: Festschrift for Sverre Grimnes*, edited by Ø. Martinsen and Ø. Jensen (Unipub forlag, Oslo, Norway, 2009).
[54] V. Méndez, D. Campos, and F. Bartumeus, *Stochastic Foundations in Movement Ecology: Anomalous Diffusion, Front Propagation and Random Searches* (Springer-Verlag, Berlin, 2013).
[55] R. Graaff and B. J. Hoenders, Telegrapher's equation for light transport in tissue with substantial absorption, in *Biomedical Optics 2008* (Optica Publishing Group, St. Petersburg, Florida, 2008), p. BSuE52.
[56] P. Broadbridge, A. D. Kolesnik, N. Leonenko, A. Olenko, and D. Omari, Spherically restricted random hyperbolic diffusion, Entropy **22**, 217 (2020).
[57] M. O. Cáceres, M. Nizama, and F. Penini, Fisher and Shanon functionals for hyperbolic diffusion, Entropy **25**, 1627 (2023).
[58] A. Compte and R. Metzler, The generalized Cattaneo equation for the description of anomalous transport processes, J. Phys. A: Math. Gen. **30**, 7277 (1997).
[59] N. Leonenko and J. Vaz, Spectral analysis of fractional hyperbolic diffusion equations with random data, J. Stat. Phys. **179**, 155 (2020).
[60] M. Nizama and M. O. Cáceres, Intermittent Kac's flights and the generalized telegrapher's equation, Phys. Rev. E **109**, 024116 (2024).
[61] E. W. Montroll and G. H. Weiss, Random walks on lattices. II, J. Math. Phys. **6**, 167 (1965).
[62] E. W. Montroll and B. J. West, On an enriched collection of stochastic processes, in *Fluctuation Phenomena*, edited by E. W. Montroll and J. L. Lebowitz (Elsevier Science, Amsterdam, 1979), pp. 61–206.
[63] B. J. West and W. Deering, Fractal physiology for physicists: Levy statistics, Phys. Rep. **246**, 1 (1994).
[64] V. M. Kenkre, E. W. Montroll, and M. F. Shlesinger, Generalized master equations for continuous-time random walks, J. Stat. Phys. **9**, 45 (1973).
[65] R. Zwanzig, From classical dynamics to continuous time random walks, J. Stat. Phys. **30**, 255 (1983).
[66] R. Zwanzig, Ensemble method in the theory of irreversibility J. Chem. Phys. **33**, 1338 (1960).
[67] S. Nakajima, On quantum theory of transport phenomena: Steady diffusion, Prog. Theor. Phys. **20**, 948 (1958).
[68] W. Feller, *An Introduction to Probability Theory and its Applications*, Vol. 2, 2nd ed. (Wiley, New York, 1971).
[69] C. R. Cox, Renewal theory, in *Monographs on Statistic and Applied Probability*, edited by C. R. Cox and D. V. Hinkley (Chapman & Hall, London, 1962).
[70] J. Masoliver, Three-dimensional telegrapher's equation and its fractional generalization, Phys. Rev. E **96**, 022101 (2017).
[71] B. D. Hughes, *Random Walk and Random Environments* (Oxford Science, Oxford, 1995), Vol. 1.
[72] I. McHardy, M. Nizama, A. A. Budini, and M. O. Cáceres, Intermittent waiting-time noises through embedding processes, J. Stat. Phys. **177**, 608 (2019).